Conformation-Specific Spectroscopy of 4-Phenyl-1-butyne and 5-Phenyl-1-pentyne

Talitha M. Selby and Timothy S. Zwier*

Department of Chemistry, Purdue University, West Lafayette, Indiana 47907-2084

Received: June 1, 2005; In Final Form: July 19, 2005

4-Phenyl-1-butyne and 5-phenyl-1-pentyne were studied by a combination of methods including resonance-enhanced-two-photon ionization, UV−UV hole-burning spectroscopy, and rotational band contour studies. There are two conformations of 4-phenyl-1-butyne observed in the expansion with their $S_1 \leftarrow S_0$ origins occurring at 37617 and 37620 cm^{-1}. MP2 and DFT calculations identify these two low energy conformations (with the acetylenic group anti or gauche with respect to the ring) and confirm that these are the only two low energy conformations anticipated to have population in them. The experimental rotational band contours of the origin bands were compared to simulations based on transition moment directions and rotational constants predicted by CIS calculations. This comparison leads to definitive assignments for the bands, with the gauche and anti conformations assigned to the red and blue-shifted conformers, respectively. Three conformations of 5-phenyl-1-pentyne were observed in the expansion with their $S_1 \leftarrow S_0$ origins occurring at 37538, 37578, and 37601 cm^{-1}. MP2 and DFT calculations predict four low energy structures arising from gauche or anti conformations about each of the Cα−Cβ and Cβ−Cγ bonds. Rotational band contour analysis was used to assign the above transitions to gauche−anti (ga), gauche−gauche (gg), and anti−gauche (ag) structures, respectively.

I. Introduction

Combustion models face a daunting task as they seek to describe the complex array of reactions that produce and destroy aromatics and polyaromatic hydrocarbons in flames and combustion engines.[1−5] Most experimental studies have rightly approached this task by studying flames involving a single fuel or a single fuel doped by a single additive.[1,2,5−10] However, combustion engines burn gasoline or diesel fuels, which are not single-component fuels but instead are complicated mixtures of hydrocarbons and additives including significant fractions of alkylbenzenes of various chain lengths. Since aromatic molecules are important precursors to soot formation, the incomplete combustion of these aromatic derivatives has been shown to be responsible for a substantial fraction of the soot/particle formation in automobile exhaust.[11]

Whatever their original source, substituted benzenes clearly play an important role in the pathways to larger PAH molecules in combustion engines and more generally in flames.[11,12] The chemical complexity of many of the substituted aromatics in fuels and fuel-rich flames necessarily opens the possibility for structural and conformational isomers. One anticipates that different structural isomers could have substantially different chemical reactivity, particularly in their abilities to form larger PAH molecules. The same may be said for conformational isomers of large flexible molecules where reacting segments often need to rearrange in order for reaction to occur.

One might have thought that the barrier heights for most simple isomerizations would be known with high accuracy from both experiment and theory. However, there is a startling disagreement between experiment and theory in numerous systems.[13] We have recently introduced the method of stimulated emission pumping−population transfer spectroscopy, which directly probes both the barriers to isomerization and relative energies of the conformational isomers of various flexible molecules.[14−18] Using this method, we would like to characterize the potential energy surfaces and the energy-dependent isomerization rates of a series of phenylalkynes of increasing complexity.

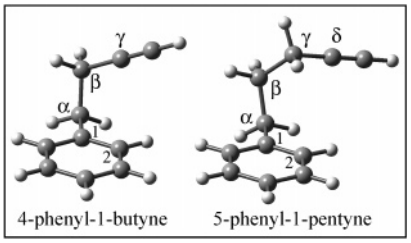

Figure 1. Pictures of 4-phenyl-1-butyne and 5-phenyl-1-pentyne with carbon atom labeling scheme shown.

The purpose of the present study is to spectroscopically characterize the low-energy conformations of two phenylalkynes, 4-phenyl-1-butyne and 5-phenyl-1-pentyne (Figure 1), to lay the groundwork for such experiments. In the following paper we also present the conformational spectroscopy of a branched-chain phenylalkyne, 3-benzyl-1,5-hexadiyne:

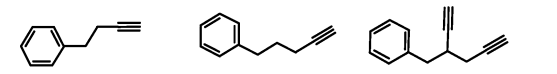

4-Phenyl-1-butyne is intriguing not only as prototypical aromatic fuel component but also as a recombination product of two resonance-stabilized radicals: benzyl and propargyl:

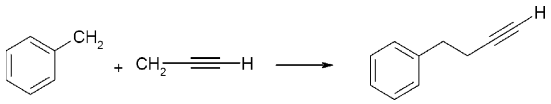

* Corresponding author. E-mail: zwier@purdue.edu. Telephone: (765) 494-5278. Fax: (765) 494-5330.

10.1021/jp0529218 CCC: $30.25
Published on Web 09/01/2005

Given the important role played by propargyl recombination as a route to benzene in flames,[19] it is worth considering the analogous reactions involving other resonance-stabilized radicals, which would be anticipated to undergo the same kind of build-up in concentration due to their unusual stability. The spectroscopic characterization of 4-phenyl-1-butyne is a necessary first step in characterizing this recombination reaction, since it is the primary recombination product anticipated.

The present spectroscopic study builds on earlier work on alkyl-substituted benzenes.[20−23] From those studies, it is known that *n*-propylbenzene has population in two low-energy conformations under expansion cooling. These conformations both have the Cα−Cβ bond perpendicular to the phenyl ring, with the terminal methyl group either anti or gauche relative to the phenyl ring. The $S_1 \leftarrow S_0$ electronic origins of these conformers occur at 37533 and 37583 cm^{-1}.[21] Early rotational band contour[21] analysis was later confirmed by high resolution[20] studies, leading to assignments of the red- and blue-shifted origins to the gauche and anti structures, respectively.

In *n*-butylbenzene, four conformations are observed in the expansion,[20,21,23] with $S_1 \leftarrow S_0$ origin transitions that come in two pairs, with gauche or anti conformations about the Cα−Cβ bond split by 60 cm^{-1} from one another (gauche red-shifted from anti), with an additional 2−3 cm^{-1} splitting due to the conformation about the Cβ−Cγ bond.[20−22] In the alkylbenzenes, the red-shifted electronic origins of gauche conformations are attributed to the interaction of the γ-methylene hydrogen with the ring.[24]

The high-resolution electronic spectroscopy of the above-mentioned alkylbenzenes also reveals that the direction of the transition dipole moment (TDM) changes from a perpendicular (*b*-type) transition in anti structures to a hybrid band type (*a*-, *b*-, and *c*-type) in gauche structures with about a 30° difference in the TDM.[25] The change in the TDM direction in going from anti to gauche structures is attributed to the off-axis nature of the gauche structure which causes a mixing of the excited-state molecular orbitals to form mixed $^1L_a/^1L_b$ states.[25] CIS calculations of these systems correctly predict these results, giving TDM directions within a few degrees of the experimental result.[25] This close connection between experimental and calculated TDM directions is exploited in the present work as well.

II. Methods

A. Experimental Details. The experimental apparatus and methods used for the spectroscopic studies have been described in detail elsewhere.[14,26,27] Here, we summarize these methods, highlighting those aspects unique to the present work. The techniques used in this work were one-color resonance-enhanced-two-photon ionization (1C-R2PI) and ultraviolet-holeburning (UVHB) spectroscopy. Additionally, 2C-R2PI was used to obtain rotational band contours and excited-state lifetimes. While 1C-R2PI provides ultraviolet spectra containing contributions from all conformers present, UVHB spectroscopy can be used to obtain UV spectra of individual conformers free from interference from one another. All UV laser experiments were performed with the frequency doubled output of a tunable Nd: YAG pumped dye laser (Coumarin 307) as UV source. Typical powers for the resonant UV laser in the 1C-R2PI and the probe laser in the UV HB experiments were ~0.2 mJ/pulse at a repetition rate of 20 Hz. In UVHB experiments, the holeburn laser power was kept sufficiently high (1.0 mJ/pulse at 10 Hz) to saturate or partially saturate the hole−burn transition. The delayed probe laser was tuned through transitions while the difference in ion signal between successive laser pulses (with and without the HB laser present) was recorded using active baseline subtraction.

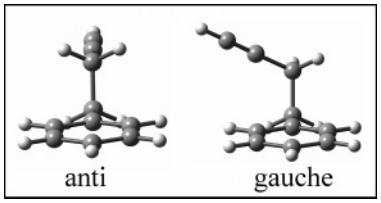

Figure 2. Pictorial summary of the two lowest energy structures of 4-phenyl-1-butyne. The anti and gauche designations refer to the position of the acetylenic group with respect to the phenyl ring.

To record rotational band contours an intracavity Etalon was used to increase the resolution of the dye laser. In this experiment, the resonant laser power was kept low (10−50 μJ/pulse) in order to avoid saturation effects, and the ionization laser power was high (1.0 mJ/pulse, $\lambda \geq 270$ nm) to increase the signal. In excited-state lifetime scans the ion signal was monitored as a function of delay time between the resonant and ionization lasers.

Both samples were heated to about 50 °C and entrained in a supersonic expansion created by expansion of a pure helium (5 bar) or 70% neon in helium mixture (3.5 bar) through a 800 μm orifice of a pulsed valve (R. M. Jordan Co.). The 4-phenyl-1-butyne and 5-phenyl-1-pentyne samples were purchased from Lancaster Synthesis Inc and used without further purification.

B. Computational Details. Initial screening of conformational structures was carried out using molecular mechanics methods with an OPLS-AA force field. Structures so identified were used as starting structures for quantum chemical calculations. Full optimizations were carried out using density functional theory (DFT) with a Becke3LYP[28,29] functional and a 6-31+G*[30] basis set. True minima were verified by the lack of imaginary frequencies in normal-mode analyses carried out at the optimized structures. To test the importance of electron correlation effects on the relative energies of the minima, full optimizations were then carried out using second-order Moller−Plesset perturbation (MP2) calculations with a cc-pVDZ[31] basis set. Finally, single point calculations with the aug-cc-pVDZ basis set[31,32] were also performed on DFT/6-31+G* and MP2/cc-pVDZ optimized structures. Configuration interaction singles (CIS)[33] and Hartree−Fock (HF) calculations with a 6-31G basis set were performed on selected minima in order to obtain predictions for the direction of the transition moment for the S_0-S_1 transitions of the conformers. These results served as input for simulations of rotational band contours in which the ground and excited-state rotational constants and transition dipole moment directions were taken from the calculations. Details of the fitting procedure are given in section III-3.

MM calculations were performed using MacroModel software.[34] DFT, MP2, HF, and CIS computations were carried out using Gaussian 98.[35] Rotational band contour simulations were performed using the JB95 software.[36]

III. Results and Analysis

A. Computational Details. 1. 4-Phenyl-1-butyne. OPLS-AA molecular mechanics calculations of 4-Phenyl-1-butyne (PB) predicted four minima within 8 kJ/mol of the global minimum. These structures were used as the starting structures for DFT optimizations. From these DFT optimizations, three unique structures resulted with only two structures within 8 kJ/mol of the global minimum. Figure 2 presents these lowest energy structures, both of which possess an out-of-plane geometry in

TABLE 1: Selected Structural Parameters and Selected Minima of PB and PP at the DFT (B3LYP/6-31+G*) Level of Theory

4-Phenyl-1-butyne						
description	τ1(C2−C1−Cα−Cβ), deg	τ2(C1−Cα−Cβ−Cγ), deg	C1−Cα, Å	*A″*, MHz	*B″*, MHz	*C″*, MHz
PB(anti)	−89.3	−180.0	1.514	4450	5997	554
PB(gauche)	−83.2	−67.1	1.514	2525	8628	740

5-Phenyl-1-pentyne							
description	τ1(C2−C1−Cα−Cβ), deg	τ2(C1−Cα−Cβ−Cγ), deg	τ3(Cα−Cβ−Cγ−Cδ), deg	C1−Cα, Å	*A″*, MHz	*B″*, MHz	*C″*, MHz
PP(ag)	−86.1	−179.5	−64.0	1.515	3082	479	436
PP(aa)	−89.3	−180.0	−180.0	1.515	3163	418	409
PP(gg)	−100.7	64.5	63.5	1.516	2220	639	552
PP(ga)	−108.2	64.3	178.5	1.517	2277	519	509

TABLE 2: Relative Energies of Selected Conformational Minima of PB and PP (in kJ/mol)

level of theory(basis set) [single point//optimized structure]	E_{rel}(PB(anti))[b]	E_{rel}(PP(ga))[c]	E_{rel}(PP(ag))[c]	E_{rel}(PP(aa))[c]
B3LYP(6-31+G*)//B3LYP(6-31+G*)]	−4.12	0.50	−1.22	−1.04
B3LYP(6-31+G*)//B3LYP(6-31+G*) + ZPE[a]	−4.05	−0.04	−1.76	−2.31
MP2(cc-pVDZ)// MP2(cc-pVDZ)	0.69	5.03	5.60	8.55
MP2(cc-pVDZ)// MP2(cc-pVDZ) + ZPE[a]	0.76	4.48	5.06	7.28
MP2(aug-cc-pVDZ)//B3LYP(6-31+G*)+ ZPE[a]	−0.92	3.96	4.71	6.17
MP2(aug-cc-pVDZ)//MP2(cc-pVDZ) + ZPE[a]	0.82	5.72	7.38	9.42

[a] Zero-point energy contributions are determined at the Becke3LYP/6-31+G* level of theory. [b] Energy relative to PB(gauche) in kJ/mol. [c] Energy relative to PP(gg) in kJ/mol.

which the beta-carbon is nearly perpendicular to the ring. These two conformers differ mainly in the dihedral angle τ2(C1−Cα−Cβ−Cγ) that specifies the position of the acetylenic group relative to the phenyl ring (see Table 1 and Figure 1). In the anti conformation, τ2 is approximately ±180°; whereas in the gauche conformation, τ2 is approximately ±60°. Selected molecular parameters and rotational constants of these two conformations of PB calculated at DFT level of theory are given in Table 1. Table 2 summarizes the calculated relative energies at DFT and MP2 levels of theory both with and without zero-point energy (ZPE) corrections. DFT calculations predict that the PB anti structure is about 4 kJ/mol more stable than the gauche structure while MP2 calculations show that the two conformers are close in energy.

2. 5-Phenyl-1-pentyne. MM calculations of 5-phenyl-1-pentyne (PP) resulted in seven minima within 21 kJ/mol of the global minimum. These structures were used as the starting structures in DFT optimizations. In the DFT optimizations, all seven starting structures minimized to distinct conformational isomers, with four structures within 8 kJ/mol of the global minimum. Figure 3 presents those four lowest energy conformations. The defining angles used to distinguish different conformations are given in Table 1 and used in the naming scheme shown in Figure 3. As in PB, the anti and gauche designations differ mainly by the dihedral angle τ2(C1−Cα−Cβ−Cγ) (see Table 1 and Figure 1). In the anti conformation, τ2 is approximately ±180°; whereas in the gauche conformation, τ2 is approximately ±60°. The second designation (anti or gauche) differs mainly in the value of the dihedral angle τ3(Cα−Cβ−Cγ−Cδ). In the anti configuration, τ3 is approximately ±180°; whereas in the gauche configuration, τ3 is approximately ±60°. Selected molecular parameters and rotational constants of these four conformations of PP calculated at DFT level of theory are given in Table 1. Table 2 summarizes the calculated relative energies at DFT and MP2 levels of theory with and without ZPE corrections. As in PB, DFT calculations predict that the PP anti structures are about 2 kJ/mol more stable than the gauche structures while MP2 predicts that the PP(gg) structure is the most stable. The MP2/aug-cc-pVDZ single-point energy calculations taken at the DFT/6-31+G* and MP2/cc-pVDZ optimized structures are consistent with one another, indicating that the difference in the results from MP2 and DFT calculations are due to the different method and not due to the basis set size.

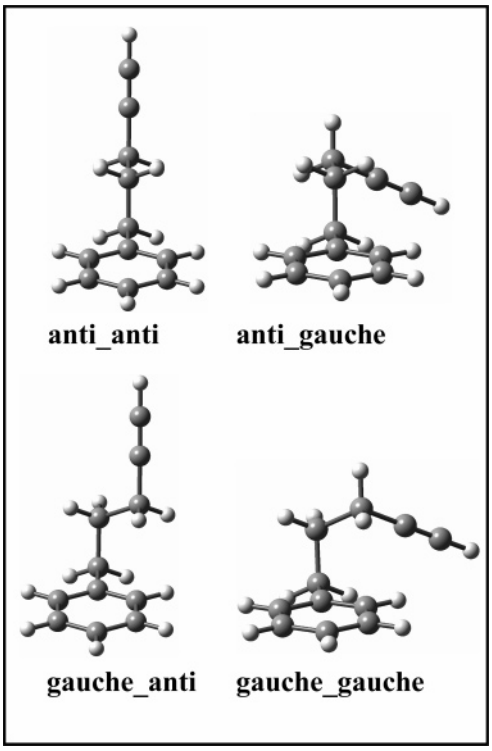

Figure 3. Pictorial summary of the four lowest energy structures of 5-phenyl-1-pentyne. The first part of the naming scheme denotes the conformation about the Cα−Cβ, and the second part that about the Cβ−Cγ bond (see Figure 1).

B. R2PI and UVHB Spectra. 1. Overview R2PI of 4-Phenyl-1-butyne and 5-Phenyl-1-Pentyne. Figure 4 presents the overview 1C-R2PI spectra of PB and PP. Not surprisingly, the spectra are very similar to the excitation spectra of the alkylbenzenes recorded by Smalley and co-workers.[22] Like most substituted benzenes, most of the Franck−Condon (FC) activity is in the ring modes, since it is the geometry of the ring that is affected most by the $\pi-\pi^*$ excitation. Shown in Figure 4 is

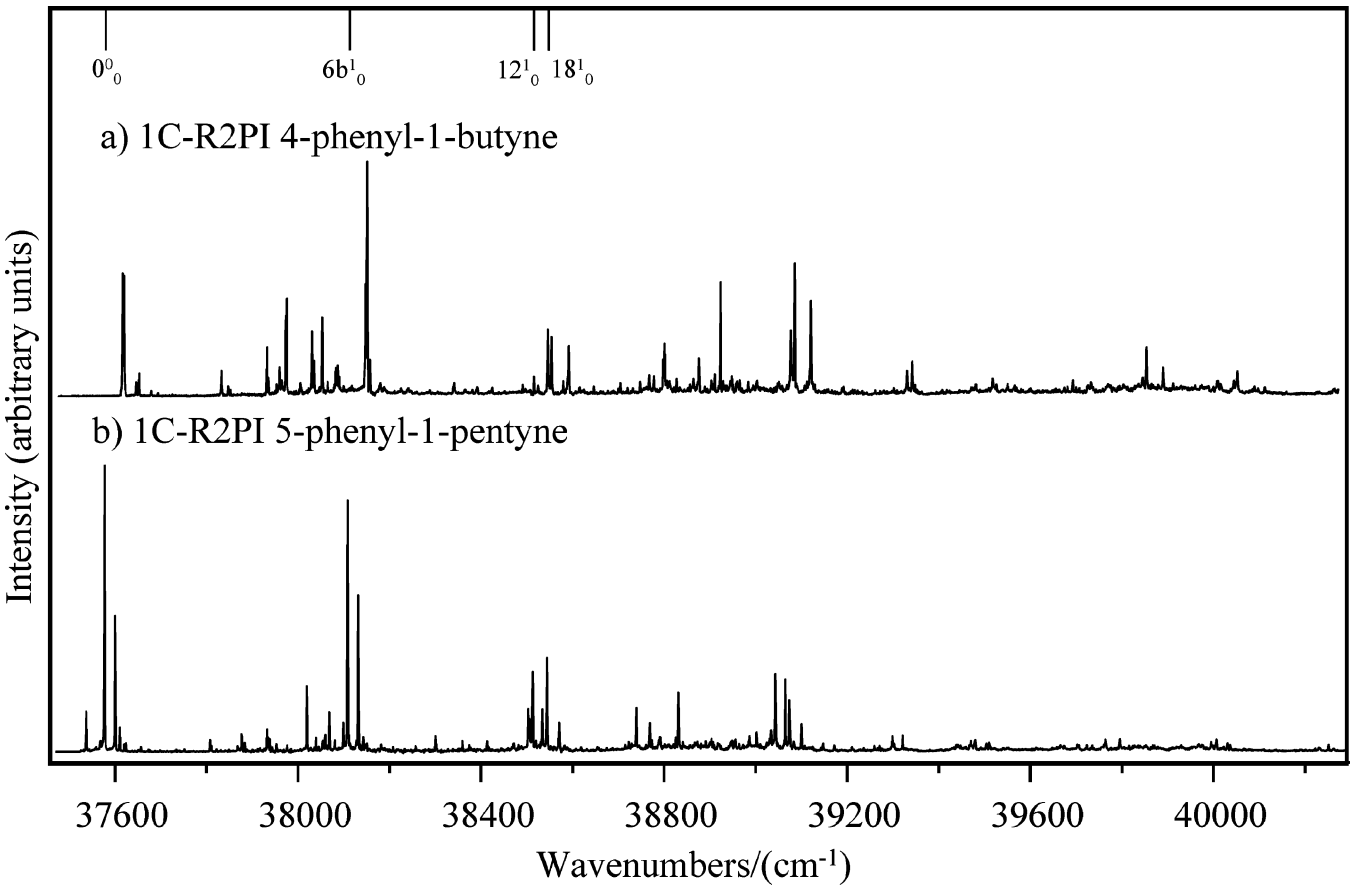

Figure 4. Overview 1C-R2PI spectra of (a) 4-phenyl-1-butyne and (b) 5-phenyl-1-pentyne with the *anti*-propylbenzene[22] origin transition and selected ring modes (Wilson notation) shown for reference above the R2PI spectra.

the origin position and selected ring modes (using Wilson notation) of anti *n*-propylbenzene for comparison.[22]

One of the interesting possibilities raised by these conformation-specific spectra is the potential for conformation-specific dynamics in the excited state. One way that such dynamics might present itself would be if there were different vibronic-specific lifetimes of the conformers in the excited state. To test this possibility, lifetimes of many of the transitions observed were obtained throughout both spectra by delaying the ionization laser relative to the laser used for the $S_1 \leftarrow S_0$ step. In all conformations of both PB and PP, the lifetimes are close to 85 ns near the origin and 55 ns about 2000 cm^{-1} above the origin with a smooth decline as the excitation energy increased. The similarity of the lifetimes at similar excitation energies throughout the spectrum indicates there is no conformational dependence of the lifetimes. This result is similar to that reported by Smalley and co-workers[37] for the alkylbenzenes where the origin transitions have fluorescence lifetimes of ~85 ns with a small decrease in lifetime as the excitation energy increases.

The fact that the S_1 lifetime is still 55 ns nearly 2000 cm^{-1}above the origin indicates that the drop-off in intensity above 2000 cm^{-1} is due primarily to a decrease in Franck−Condon factors for these transitions (Figure 4).

2. UVHB of 4-Phenyl-1-butyne. Parts a and b of Figure 5 present the 1C-R2PI spectra of PB expanded in the origin region (Figure 5a) and at an intermediate scale which focuses on the first 550 $cm^{-1}$of the spectrum (Figure 5b). The UHVB spectra of conformers PB(A) and PB(B) (Figure 5c and d) are shown below the R2PI spectrum (Figure 5b). All transitions observed in the R2PI spectrum are accounted for by the UVHB spectra of PB(A) and PB(B); thus, we conclude there are two conformations of PB present in the expansion.

3. Rotational Band Contour Analysis of 4-Phenyl-1-butyne. Parts a and b of Figure 6 (top traces) present the rotational band contour spectra of the origin bands of PB(A) and PB(B), respectively. Since the experimental traces are not fully resolved, it is not possible to obtain a completely unconstrained best fit. Instead, simulations based on ab initio predictions (bottom traces) were followed by best "fits" that make small changes about the ab initio predicted values (middle traces). The rotational parameters from HF(6-31G) and CIS(6-31G) used in the simulations and "fits" are given in Table 3.

The procedure for the simulations and fits in this work is very similar to the procedure used by Dickinson and co-workers in the rotational analysis of *n*-propylbenzene and *n*-butylbenzene.[21] To obtain the simulations, the experimental traces were preliminarily assigned to a conformation, and the ab initio values for the ground and excited-state rotational constants and TDM were used for each simulation at an assumed rotational temperature and resolution. The temperatures and resolutions were then adjusted to match the experimental traces. To obtain a better fit, first the experimental values of $(A - B_{avg})'$ and $(A - B_{avg})''$ (where $B_{avg} = 1/2(B + C)$) were calculated from the ^pQ and ^rQ subband head spacings (as the experimental resolution allowed). Then the A' and A'' rotational constants were adjusted to match the experimental $(A - B_{avg})'$ and $(A - B_{avg})''$ values while the B', B'', C', and C'' values were held at the ab initio values. If multiple sets of A' and A'' rotational constants gave equally good fits, then only A' was adjusted while A'' was held at the ab initio value. Last, attempts were made to adjust the TDM in hybrid bands to obtain better relative intensities of the subband heads; however, if no better fits were obtained by doing this, then all TDM compositions were held at the ab initio values.

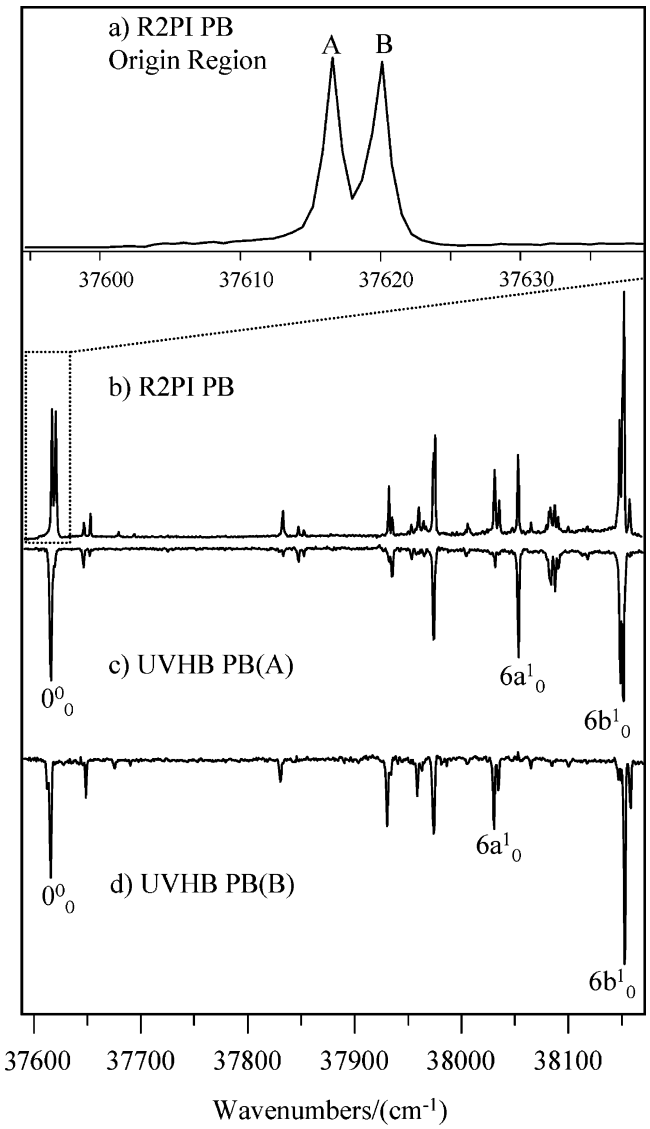

Figure 5. (a) 1CR2PI spectrum of PB expanded in the origin region, (b) spectrum at an intermediate scale that spans the first 550 cm^{-1} of the spectrum, and (c, d) UVHB spectra of conformers (c) PB(A) and (d) PB(B). The 0^0_0, $6a^1_0$, and $6b^1_0$ transitions are labeled.

The rotational band contour for the origin band of PB(B) is unmistakably a perpendicular-type transition and is assigned to the anti conformation (Figure 6b). Ab initio simulations show the anti conformer is a perpendicular transition with composition $\mu_a^2:\mu_b^2:\mu_c^2 = 0:100:0$ and with a calculated $(A - B_{avg})'' = 0.129$ (Table 3). The experimental value of $(A - B_{avg})''$ is equal to 0.13 cm^{-1} (Table 3), consistent with ab initio calculations of the anti conformation (Table 3). Because of symmetry restrictions, the TDM must necessarily lie along a single inertial axis, and hence was held fixed as pure *b*-type.

The rotational band contour for PB(A) possesses a significant Q-branch, indicating the presence of significant *a*-character to the band. Simulations based on the CIS predictions show the gauche conformer to be a hybrid-band with composition $\mu_a^2:\mu_b^2:\mu_c^2 = 27:36:37$ and with a calculated $(A - B_{avg})'' = 0.0582$ (Table 3). This prediction does a remarkably good job of matching the experimental result.

In the case of the gauche conformer there were multiple sets of A' and A'' that gave equally good fits to the experimental contour of PB(A). Thus, only A' was adjusted while A'' was held at the ab initio value. The TDM composition ($\mu_a^2:\mu_b^2:\mu_c^2 = 27:36:37$) at the ab initio value also gave a good match to the experimental contour. However, small changes could be made in the TDM composition to obtain equally good fits. The estimated error in the TDM composition for the gauche conformer is about 5%.

TABLE 3: Calculated[a] and Experimental Ground and Excited State Rotational Parameters of the Anti and Gauche Conformers of 4-phenyl-1-butyne Used in Rotational Band Contour Simulations and Best Fits

Calculation		
parameter	gauche	anti
A'' (MHz)	2557	4452
B'' (MHz)	875	60‘5
C'' (MHz)	749	559
ΔA (MHz)	−76	−120
ΔB (MHz)	−11	−3
ΔC (MHz)	−4	−4
$(A - B_{avg})''$ (cm^{-1})	0.0582	0.129
$\mu_a^2:\mu_b^2:\mu_c^2$	27:36:37	0:100:0
Experiment		
parameter	PB(A)	PB(B)
$(A - B_{avg})''$ (cm^{-1})	0.0582[b]	0.13(2)[c]
ΔA (MHz)	−102(7)[c]	−210(14)[c]
$\mu_a^2:\mu_b^2:\mu_c^2$	27:36:37[d]	0:100:0[b]
T (K)	3.4(2)[c]	1.6(1)[c]
fwhm (cm^{-1})	0.09(1)[c]	0.09(1)[c]

[a] HF/6-31G and CIS/6-31G levels of theory. [b] Held fixed at ab initio values. [c] Estimated experimental error shown in parentheses as the error associated with the last significant digit. [d] The estimated error in the TDM is about 5%.

4. UVHB of 5-Phenyl-1-pentyne. Parts a and b of Figure 7 present the 1C-R2PI spectra of PP expanded in the origin region (Figure 7a) and over a range that extends through the $6b^1_0$ transitions of each conformer (Figure 7b). The UHVB spectra of conformers PP(A) and PP(B) (Figure 7, parts c and d) are shown below the R2PI spectrum (Figure 7b). Most transitions in the R2PI spectrum are accounted for by conformers PP(A) and PP(B). Conformer PP(X) was identified through the transitions not accounted for by the UVHB spectra of conformers PP(A) and PP(B). The UVHB spectra of PP(X) (not shown) were obtained by hole-burning on its origin transition, but only tuning the probe laser over regions of unidentified transitions. Four transitions of PP(X) were found in this way. The UVHB spectra of PP(X) were not taken over the entire region because the noise from the large signal of the other conformers was of the same magnitude as the PP(X) signal. All transitions observed in the R2PI spectrum are accounted for by the UVHB spectra of PP(A), PP(B), and PP(X).

Thus, we conclude that there are three conformations of PP present in the expansion with their origin transitions occurring at 37538, 37578, and 37601 cm^{-1} for conformers PP(X), PP(A), and PP(B), respectively. To make conformational assignments to these conformers, the partially resolved rotational spectra of the origin bands were recorded.

5. Rotational Band Contour Analysis of 5-Phenyl-1-Pentyne. a. Gauche Conformations. Parts a and b of Figure 8 (top traces) present the rotational band contour spectra of the origin bands of PP(X) and PP(A), respectively. Simulations from ab initio calculations and best “fits” are shown in the bottom and middle traces of Figure 8, respectively. The rotational parameters from HF(6-31G) and CIS(6-31G) used in the simulations and “fits” are given in Table 4. The PP(A) and PP(X) band contours were best fit with resolutions of 0.07 and 0.09 cm^{-1} and temperatures of 1.4 and 1.8 K, respectively. The difference in the experimental resolution may be due to saturation affects.

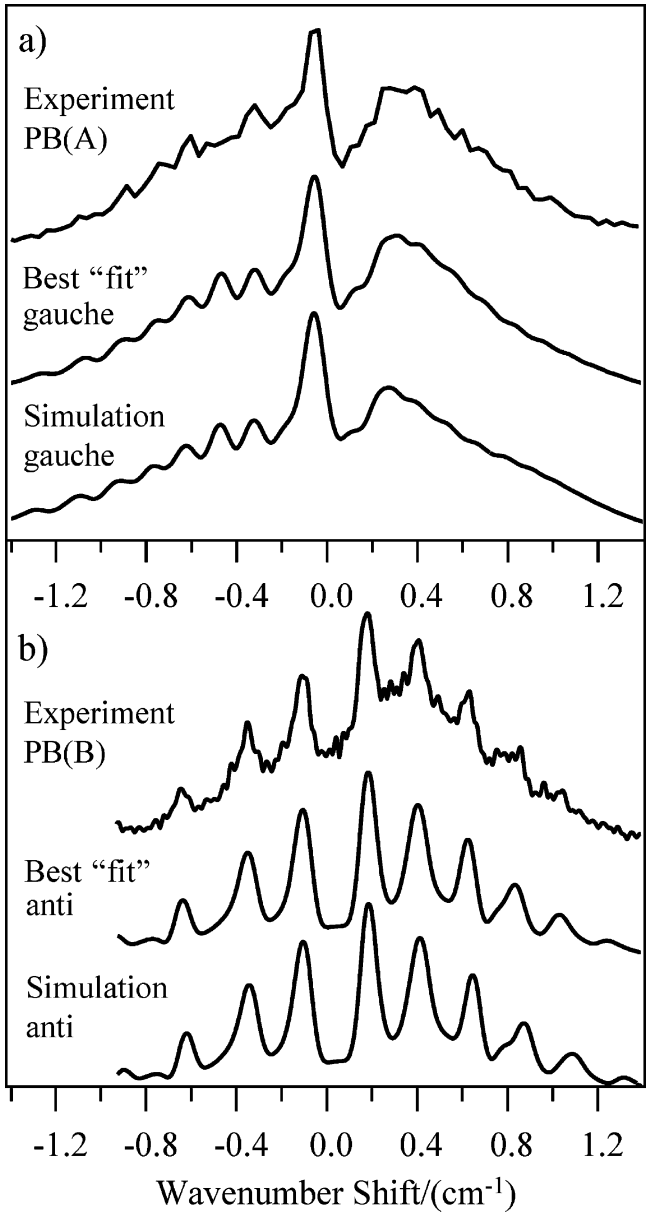

Figure 6. Top traces: 4-Phenyl-1-butyne experimental rotational band contour for (a) PB(A) and (b) PB(B). Bottom traces: rotational band contour simulation based on ab initio predictions for the rotational constants and transition dipole direction (Table 3) for 4-phenyl-1-butyne conformations (a) gauche and (b) anti. Middle traces: fits to experimental data of (a) gauche to PB(A) and (b) anti to PB(B) where A'' and A' were varied to better fit the experimental data with all other parameters held at the ab initio values (Table 3). Values used in these fits are summarized in Table 3.

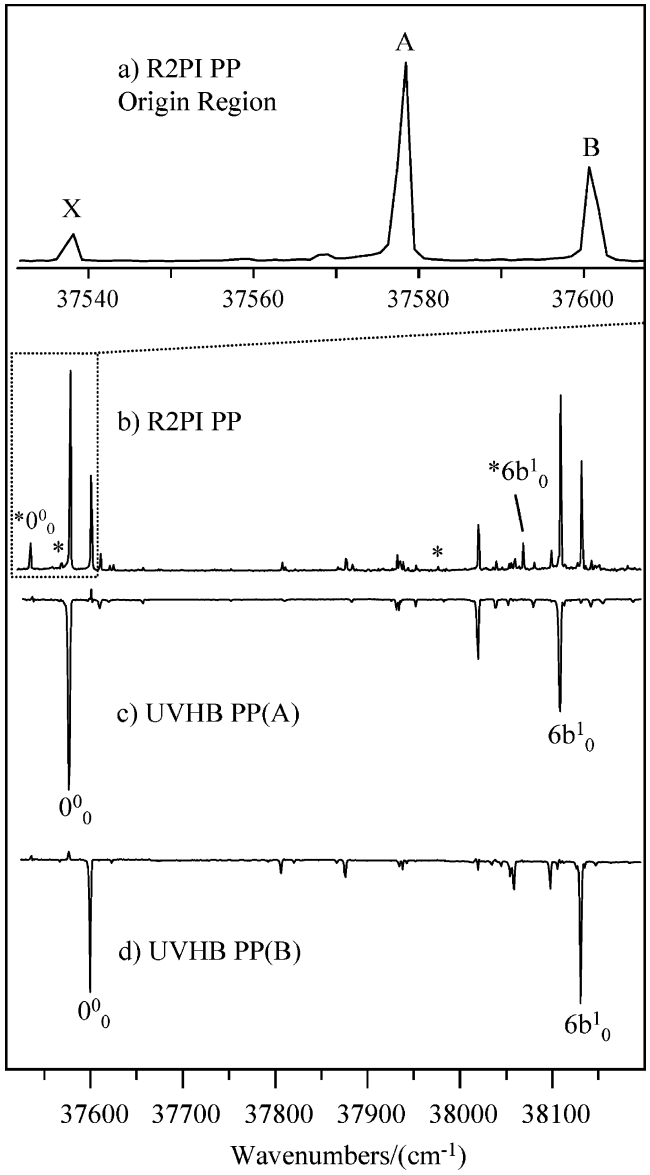

Figure 7. (a) 1CR2PI spectrum of PP expanded in the origin region, (b) spectrum at an intermediate scale that spans the first 550 cm^{-1} of the spectrum, and (c, d) UVHB spectra of conformers (c) PP(A) and (d) PP(B). Conformer PP(X) was only hole-burned with the probe laser tuned locally over transitions not accounted for by the holeburning of conformers PP(A) and PP(B). These four transitions belonging to PP(X) are marked with an asterisk in the R2PI spectrum. The 0^0_0 and $6b^1_0$ transitions are labeled for each conformation.

PP(X) (Figure 8a) is unmistakably a perpendicular-type transition. The experimental value of $(A - B_{avg})''$ (0.06 cm^{-1}) (Table 4) is consistent with a gauche conformation. Both the PP(gg) and PP(ga) conformers are calculated to have similar $(A - B_{avg})''$ values; however, only the PP(ga) structure is predicted to have a perpendicular transition ($\mu_a^2:\mu_b^2:\mu_c^2 = 18:0:82$) (Table 4). Accordingly, we assign PP(X) to the PP(ga) conformer. A slightly better match to the experimental contour subband head intensities was obtained by adjusting the TDM composition to $\mu_a^2:\mu_b^2:\mu_c^2 = 10:0:90$. The appearance of a predominantly *c*-type transition is due to the reorientation of the inertial axes in this conformation.

PP(A) (Figure 8b) resembles a parallel-type band. Additionally, the experimental value of $(A - B_{avg})'' = 0.05$ cm^{-1} (Table 4) is consistent with a gauche conformation. Ab initio simulations show the PP(gg) conformer is a hybrid-band with composition $\mu_a^2:\mu_b^2:\mu_c^2 = 57:37:6$ and a calculated $(A - B_{avg})'' = 0.0543$ cm^{-1} (Table 4). Thus, we assign PP(A) to the PP(gg) conformation. A better match to the experimental P, Q, and R branch relative intensities was obtained by adjusting the TDM to $\mu_a^2:\mu_b^2:\mu_c^2 = 29:38:33$. The estimated error in the TDM composition for the gg conformer is about 5%.

b. Anti Conformations. The top traces in parts a and b of Figure 9 present the experimental rotational band contour of the origin band of PP(B). Simulations from ab initio calculations and best "fits" to (a) PP(ag) and (b) PP(aa) are shown in the bottom and middle traces of Figure 9, respectively. The rotational parameters from HF(6-31G) and CIS(6-31G) used in the simulations and fits are given in Table 4. A resolution of 0.06 cm^{-1} and temperature of 1.5 K was used in all the simulations and fits shown in Figure 9.

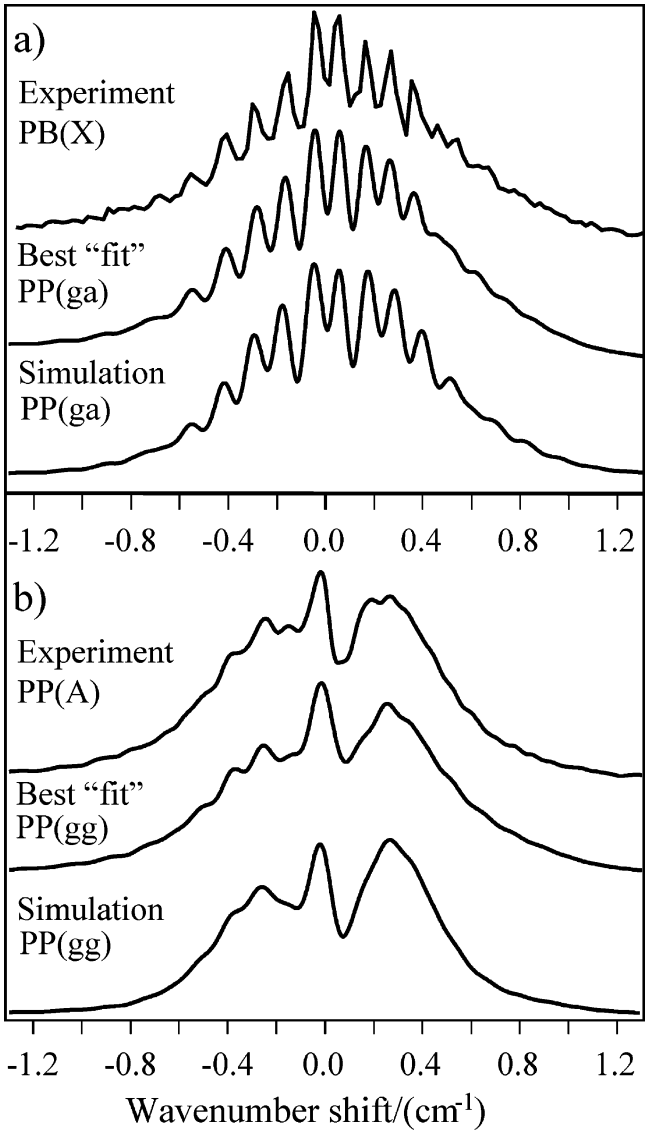

Figure 8. Top traces: 5-phenyl-1-pentyne experimental rotational band contour for (a) PP(X) and (b) PP(A). Bottom traces: rotational band contour simulation from ab initio calculations (Table 4) for 5-phenyl-1-pentyne conformations (a) ga and (b) gg. Middle traces: Fits to experimental data of (a) ga to PP(X) and (b) gg to PP(A) where A'' and A' were varied to better fit the experimental data and all other parameters were held at the ab initio values (Table 4). Values used in "fit" are summarized in Table 4.

The experimental contour of PP(B) is a perpendicular-type transition. The experimental $(A - B_{avg})''$ value ($\sim$0.08 cm^{-1}) is consistent with an anti structure. The PP(ag) and PP(aa) structures have calculated $(A - B_{avg})''$ values equal to 0.0884 and 0.0917 cm^{-1}, respectively.

On the basis of this close similarity, it is difficult to make a firm assignment for PP(B) to one of these conformations. Nevertheless, close examination of Figure 9 reveals the subband head spacings of the PP(ag) structure matches the experimental contour of PP(B) better than the PP(aa) structure. A careful grid search of slightly different A' and A'' (where the other rotational constants were held at the PP(aa) calculated values) revealed that no combination of A' and A'' gave a better fit of PP(B) to PP(aa) than shown in Figure 9. The relative intensities of the subband heads in the experimental contour of PP(B) also match the PP(ag) fitted contour better than the PP(aa) fitted contour. Hence, we tentatively assign PP(B) to the PP(ag) conformer.

TABLE 4: Calculated[a] and Experimental Ground and Excited State Rotational Parameters of Selected Conformers of 5-Phenyl-1-pentyne Used in Rotational Band Contour Simulations and Best Fits

Calculated				
parameter	ga	gg	ag	aa
A'' (MHz)	2277	2232	3113	3161
B'' (MHz)	519	649	484	417
C'' (MHz)	509	560	440	409
$(A - B_{avg})''$ (cm^{-1})	0.0588	0.0543	0.0884	0.0917
ΔA (MHz)	−32	−53	−81	−78
ΔB (MHz)	3	−3	−2	3
ΔC (MHz)	3	−3	−3	2
μ_a^2:μ_b^2:μ_c^2	18:0:82	57:37:6	5:92:3	0:100:0
Experimental				
parameter	PP (X) to ga	PP (A) to gg	PP (B) to ag	PP(B) to aa
$(A - B_{avg})''$ (cm^{-1})	0.06(1)[c]	0.05(1)[c]	0.08(2)[c]	0.08(2)[c]
ΔA (MHz)	−82(6)[c]	−61(4)[c]	−108(8)[c]	−105(7)[c]
μ_a^2:μ_b^2:μ_c^2	10:0:90[d]	29:38:33[d]	5:92:3[d]	0:100:0[b]
T (K)	1.4(1)[c]	1.8(1)[c]	1.5(1)[c]	1.5(1)[c]
fwhm (cm^{-1})	0.07(1)[c]	0.09(1)[c]	0.06(1)[c]	0.06(1)[c]

[a] HF/6-31G and CIS/6-31G levels of theory. [b] Held fixed at ab initio values. [c] Estimated experimental error shown in parentheses as the error associated with the last significant digit. [d] The estimated error in the TDM is about 5%.

The calculated TDM composition (μ_a^2:μ_b^2:μ_c^2 = 5:92:3) gave the best fit to the experimental contour.

By process of elimination, it is the PP(aa) conformer that is missing from the spectrum. The absence of this conformer in the expansion is consistent with MP2 energy calculations which predict it to be the highest in energy out of the four lowest-energy calculated structures. A further discussion of the conformational populations is given in the Supporting Information.

6. Vibronic Structure in 4-Phenyl-1-butyne and 5-Phenyl-1-pentyne. With the PB and PP conformational assignments in hand, the vibronic structure can be discussed. A table of the experimental frequencies and intensities and calculated frequencies (CIS/6-31G) for both molecules is given in the Supporting Information. The 0^0_0, $6a^1_0$, $6b^1_0$ transitions are labeled for both conformations of PB in Figure 5, and the 0^0_0 and $6b^1_0$ transitions are labeled for the three conformations of PP in Figure 7. These transitions were assigned based on comparisons with *n*-propylbenzene.[22] The origins of PB(gauche) and PB(anti) occur at 37617 and 37620 cm^{-1}, respectively. Unlike the anti and gauche conformers of *n*-propylbenzene, there is only a 3 cm^{-1} shift between the two conformations of PB. As expected the $6b^1_0$ transitions of both conformations are within a few wavenumbers of each other occurring at 531/534 and 532 cm^{-1} for PB(gauche) and PB(anti), respectively. Like in the alkylbenzenes, the $6a^1_0$ transitions show more sensitivity to conformation than the $6b^1_0$ transitions, occurring at 436 and 410 cm^{-1} for PB(gauche) and PB(anti), respectively. There is also only a slight variation in the chain-ring torsion at 30 and 33 cm^{-1} in PB(gauche) and PB(anti), respectively. In PB(anti), this torsional mode has a$''$ symmetry. According to CIS(6-31G) calculations, the S_1 state has A'' symmetry and the S_0-S_1 transition moment lies along the *b*-axis. Thus, only totally symmetric vibrations (a$'$) are predicted to have allowed fundamentals. The appearance of a nontotally symmetric fundamental indicates it must be vibronically induced. The greater intensity of the $6b^1_0$ transition than the 0^0_0 transition in PB(anti) is further evidence for some conformation specificity to the vibronic coupling with a second close-by excited state.

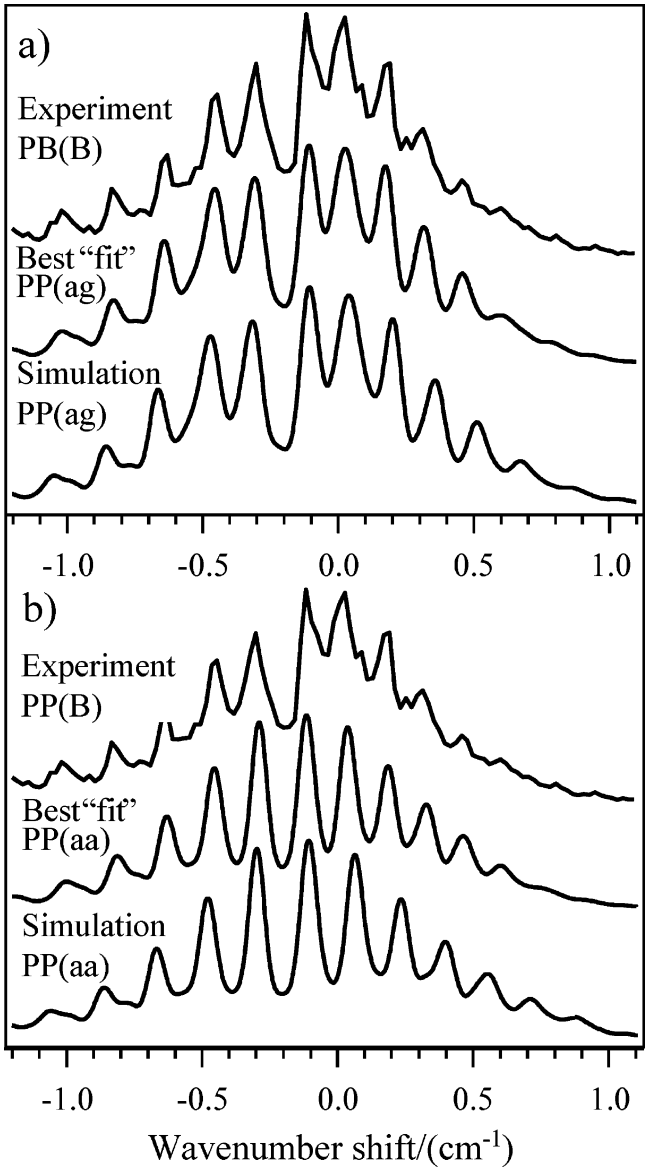

Figure 9. Top traces: 5-phenyl-1-pentyne experimental rotational band contour of PP(B). Bottom traces: rotational band contour simulation from ab initio calculations (Table 4) for 5-phenyl-1-pentyne conformations (a) ag and (b) aa. Middle traces: Fits to experimental data of (a) ag to PP(B) and (b) aa to PP(B) where A'', A', and $\mu_a^2:\mu_b^2:\mu_c^2$ were varied to better fit the experimental data and all other parameters were held at the ab initio values (Table 4). Values used in "fit" are summarized in Table 4.

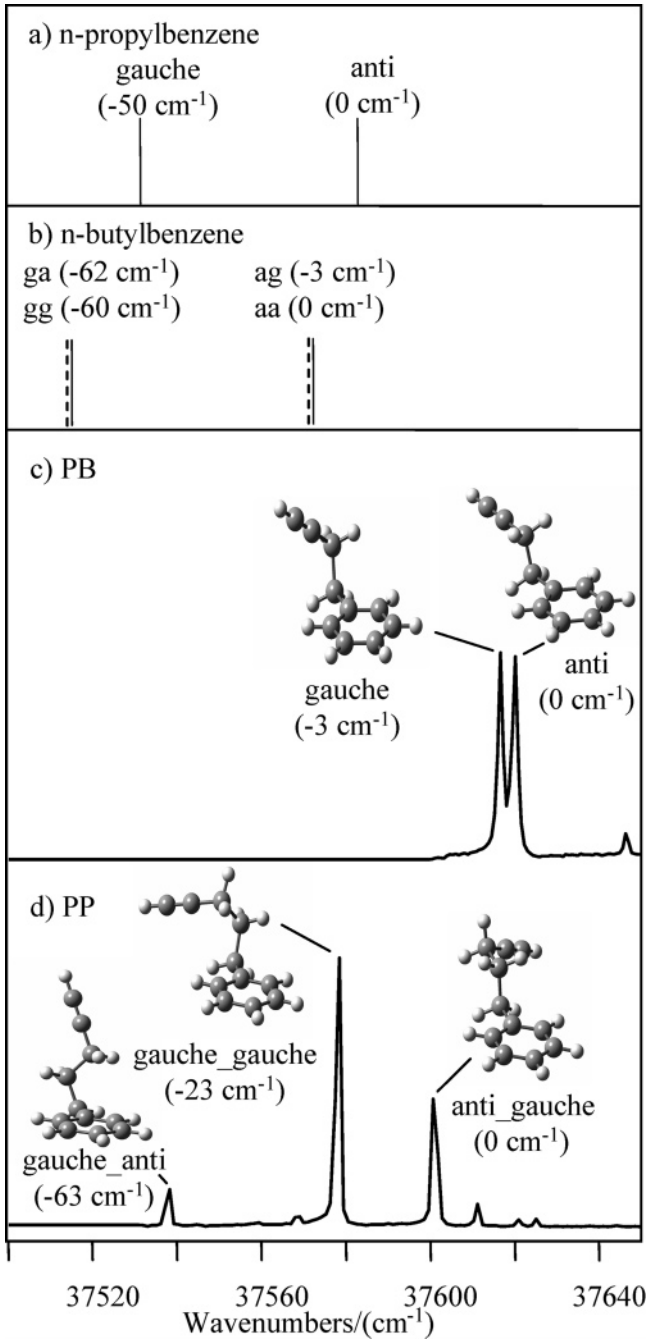

Figure 10. Summary of conformational assignments of (c) PB and (d) PP with the origin positions of (a) the two conformers of *n*-propylbenzene and (b) the four conformers of *n*-butylbenzene shown for comparison.[20−22] The relative origin positions of each conformation, reported in wavenumbers relative to the highest frequency transition, are also labeled for reader reference.

The origins of PP(ga), PP(gg), and PP(ag) occur at 37538, 37578, and 37601 cm^{-1}, respectively. Similar to PB, the $6b^1_0$ transitions occur at 530−531 cm^{-1} above the origin, and the chain-ring torsions occur 24−33 cm^{-1} above the origin. The lower symmetry of PP makes these torsion fundamentals allowed. The changes in frequency of the chain-ring torsional fundamentals follow the predictions of the calculations based on the assignments from the rotational band contours, providing another confirmation of the assignments (see Supporting Information). The $6a^1_0$ transition is not easily identified as its frequency and intensity tends to shift around in the different conformations. Assignments to the other modes in PB and PP must await dispersed fluorescence studies.

IV. Discussion

A combination of supersonic expansion cooling and laser-based double resonance spectroscopy have been used to record isomer-specific ultraviolet spectra of the conformational isomers of 4-phenyl-1-butyne (PB) and 5-phenyl-1-pentyne (PP). Ultraviolet hole-burning spectroscopy determined that two conformational isomers of PB and three conformational isomers of PP are present in the expansion. The rotational band contours proved to be the most helpful in making conformational assignments in both PB and PP.

The final conformational assignments of PB and PP are summarized in Figure 10 with the results of *n*-propylbenzne and *n*-butylbenzene shown for comparison.[20−22] After analysis of the rotational band contours we make the following assignments: PB(A) to PB(gauche), PB(B) to PB(anti), PP(X) to PP(ga), PP(A) to PP(gg), and PP(B) to PP(ag). Armed with

these assignments, it is worthwhile to compare the present results on PB and PP with the results on *n*-propylbenzene and *n*-butylbenzene in order to assess the effect of the terminal acetylenic group on the spectroscopy and conformational preferences.[20−22]

A. The Conformation Dependence of the Electronic Frequency Shift. In previous work on *n*-propylbenzene and *n*-butylbenzene,[20−22] it has been established that the position of Cγ (Figure 1) plays a crucial role in the observed electronic frequency shift. When it is anti with respect to the ring, the electronic origin occurs near 37580 cm^{-1}, but when it is in the gauche position where the γ-hydrogen can interact with the π cloud, the band is shifted to the red by up to 60 cm^{-1} (Figure 10a-b). In PB, Cγ is part of the acetylenic group, and hence the gauche conformer does not have a γ-hydrogen interacting with the π cloud of the phenyl ring. Instead, the alkyl chain is replaced by the acetylenic group, which is linear and hence points up away from the ring. It is unclear whether it is simply a lack of an interaction that places the origin transition of the gauche isomer so close to its anti counterpart, or whether the two π clouds interact to produce a blue shift from its Cγ alkyl position. The latter scenario seems at odds with expectation based on an excimer-like interaction between the groups, which should produce a red shift in the excited state. In the end, the observed consequence is that the $S_1 \leftarrow S_0$ origins for gauche and anti conformers of PB (Figure 10c) occur at 37617 and 37620 cm^{-1}, split by only 3 cm^{-1} from one another and pushed to the blue edge of the "anti" region of the alkylbenzenes spectra.

In PP, Cγ is part of the alkyl chain. As shown in Figure 10d, the $S_1 \leftarrow S_0$ origin transitions for the gauche structures are shifted to the red, with the PP(ga) configuration shifted by 63 cm^{-1} from the PP(ag) configuration, much as occurs for the anti and gauche conformers in the *n*-propylbenzene and *n*-butylbenzene.[20−22] Finally, the PP(gg) origin is 40 cm^{-1} blue-shifted from the PP(ga) conformation in PP, unlike the two corresponding gauche conformer origins of *n*-butylbenzene which are found within 2 cm^{-1} of one another (Figure 10b). The observed blue-shift of the PP(gg) origin in PP suggests that the C≡CH group π cloud is interacting with the phenyl ring π cloud in this configuration, partially counteracting the effect of the Cγ CH_2 group.

B. The Conformation Dependence of the Transition Moment. One of the intriguing aspects of the present results is something these alkynylbenzenes share with a number of other singly substituted benzenes; namely, the sensitivity of the direction of the transition dipole moment to the conformation of the substituent. This sensitivity was first exploited by Simons and co-workers in making conformational assignments based on changes in the shape of the partially resolved rotational band contours, much as was done in the present work. The explanation for this sensitivity is by now well-documented. As Pratt and co-workers[20,25,38] have pointed out, in symmetric mono-substituted benzenes (i.e., phenylacetylene and anti-propylbenzene) the TDM lies along the *b*-axis, and there is a normal ordering of states where ^1L_b lies below ^1L_a. In substituted benzenes with off axis substituents (i.e., gauche alkylbenzenes) the TDM lies between the *a* and *b* axes (of the benzene ring). This reorientation of the TDM is attributed to the mixing of the excited-state MOs (LUMO and LUMO+1) where the new excited-state LUMO and LUMO+1 are no longer symmetric and antisymmetric, respectively, about the *a* and *b* axes. As a result the excited state is a mixture of ^1L_a and ^1L_b. Given the many deficiencies of CIS calculations, it is a remarkable achievement that the CIS calculations correctly predict the directions of the TDM in these conformers within 5° or so.

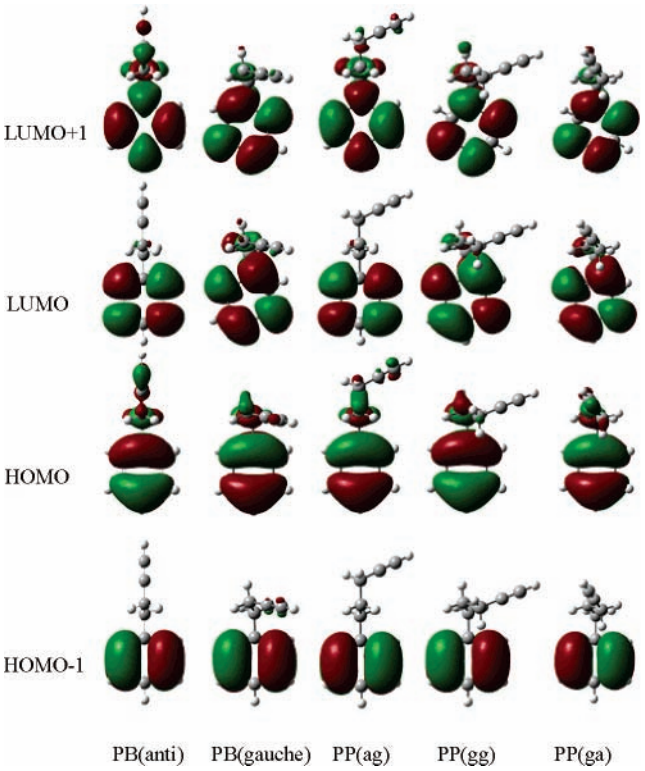

Figure 11. Molecular orbitals involved in the $\pi \rightarrow \pi^*$ transition of selected conformations of PB and PP.

The PB and PP MOs (CIS/6-31G) involved in the $S_1 \leftarrow S_0$ transition are shown in Figure 11. As anticipated, the LUMO and LUMO+1 are distorted away from the axes parallel or perpendicular to the point of substitution in all the gauche conformations. This is consistent with the observed mixed type TDM in all gauche conformers. In PB(anti) the TDM is 100% B type. In PP(ag) there is a very small *A* contribution due to the slight asymmetry associated with the off-axis position of the terminal acetylenic group. As shown in Figure 11, the LUMO and LUMO+1 for PP(ag) are very nearly symmetric and antisymmetric, respectively, about the *a* and *b* axes.

V. Conclusions

The present work has characterized the conformation-specific ultraviolet spectroscopy of 4-phenyl-1-butyne and 5-phenyl-1-pentyne. These results serve as a necessary foundation for planned experiments that will focus on the isomerization dynamics of these molecules. These experiments utilize stimulated emission pumping (SEP) to excite single "reactant" conformations early in the supersonic expansion to well-defined initial internal energies, followed by detection of single "product" conformations downstream in the expansion. This provides a means to measure the energy thresholds separating specific $X \rightarrow Y$ conformer pairs on the potential energy surface. We hope to use these methods to measure the fractional populations of the conformers, their relative conformational energies, and the energy barriers that separate them.

The following paper describes analogous conformation-specific ultraviolet and infrared spectroscopy of 3-benzyl-1, 5-hexadiyne, which also is a candidate for studies of its isomerization dynamics.

Acknowledgment. The authors gratefully acknowledge the support of the Department of Energy Basic Energy Sciences, Division of Chemical Sciences under Grant No. DE-FG02-96ER14656.

Supporting Information Available: Tables of the he frequencies and intensities of the transitions observed in the R2PI spectra of PB and PP and calculated frequencies (CIS/6-31G) with brief descriptions of the vibrational modes and text giving a discussion of the observed conformational populations compared to the computed relative energies of the conformers. This material is available free of charge via the Internet at http://pubs.acs.org.

References and Notes

(1) Babushok, V. I.; Tsang, W.; McNesby, K. L. *Proc. Combust. Inst.* **2003**, *29*, 2315.

(2) Carriere, T.; Westmoreland, P. R.; Kazakov, A.; Stein, Y. S.; Dryer, F. L. *Proc. Combust. Inst.* **2003**, *29*, 1257.

(3) Frenklach, M. *Phys. Chem. Chem. Phys.* **2002**, *4*, 2028.

(4) Richter, H.; Howard, J. B. *Phys. Chem. Chem. Phys.* **2002**, *4*, 2038.

(5) Westbrook, C. K.; Pitz, W. J.; Boercker, J. E.; Curran, H. J.; Griffiths, J. F.; Mohamed, C.; Ribaucour, M. *Proc. Combust. Inst.* **2003**, *29*, 1311.

(6) Lindstedt, P.; Maurice, L.; Meyer, M. *Faraday Discuss.* **2001**, *119*, 409.

(7) McEnally, C. S.; Pfefferle, L. D.; Westmoreland, P. R.; Homann, K. H.; Pope, C. *Proc. Combust. Inst.* **2000**, *28*, 2569.

(8) McEnally, C. S.; Pfefferle, L. D.; Robinson, A. G.; Zwier, T. S. *Combust. Flame* **2000**, *123*, 344.

(9) Anderson, H.; McEnally, C. S.; Pfefferle, L. D. *Proc. Combust. Inst.* **2000**, *28*, 2577.

(10) Roesler, J. F.; Martinot, S.; McEnally, C. S.; Pfefferle, L. D.; Delfau, J. L.; Vovelle, C. *Combust. Flame* **2003**, *134*, 249.

(11) Tancell, P. J.; Rhead, M. M.; Pemberton, R. D.; Braven, J. *Fuel* **1996**, *75*, 717.

(12) Roubaud, A.; Lemaire, O.; Minetti, R.; Sochet, L. R. *Combust. Flame* **2000**, *123*, 561.

(13) Speakman, L. D.; Papas, B. N.; Woodcock, H. L.; Schaefer, H. F., III. *J. Chem. Phys.* **2004**, *120*, 4247.

(14) Selby, T. M.; Clarkson, J.; Mitchell, D.; Fitzpatrick, J. A. J.; Lee, H. D.; Pratt, D. W.; Zwier, T. S. *J. Phys. Chem. A* **2005**, *109*, 4484.

(15) Dian, B. C.; Clarkson, J. R.; Zwier, T. S. *Science* **2004**, *303*, 1169.

(16) Clarkson, J. R.; Dian, B. C.; Moriggi, L.; DeFusco, A.; McCarthy, V.; Jordan, K. D.; Zwier, T. S. *J. Chem. Phys.* **2005**, *122*, 214311.

(17) Clarkson, J. R.; Baquero, E.; Zwier, T. S. *J. Chem. Phys.* **2005**, *122*, 214312.

(18) Clarkson, J. R.; Baquero, E.; Shubert, V. A.; Myshakin, E.; Jordan, K. D.; Zwier, T. S. *Science* **2005**, *307*, 1443.

(19) Miller, J. A.; Klippenstein, S. R. *J. Phys. Chem. A* **2003**, *107*, 7783.

(20) Borst, D. R.; Joireman, P. W.; Pratt, D. W.; Robertson, E. G.; Simons, J. P. *J. Chem. Phys.* **2002**, *116*, 7057.

(21) Dickinson, J. A.; Joireman, P. W.; Kroemer, R. T.; Robertson, E. G.; Simons, J. P. *J. Chem. Soc., Faraday Trans.* **1997**, *93*, 1467.

(22) Hopkins, J. B.; Powers, D. E.; Smalley, R. E. *J. Chem. Phys.* **1980**, *72*, 5039.

(23) Mate, B.; Suenram, R. D.; Lugez, C. *J. Chem. Phys.* **2000**, *113*, 192.

(24) Hopkins, J. B.; Powers, D. E.; Mukamel, S.; Smalley, R. E. *J. Chem. Phys.* **1980**, *72*, 5049.

(25) Kroemer, R. T. L.; K. R.; Dickinson, J. A.; Robertson, E. G.; Simons, J. P.; Borst, D. R.; Pratt, D. W. *J. Am. Chem. Soc.* **1998**, *120*, 12573.

(26) Arrington, C. A.; Ramos, C.; Robinson, A. D.; Zwier, T. S. *J. Phys. Chem. A* **1998**, *102*, 3315.

(27) Stearns, J. A.; Zwier, T. S. *J. Phys. Chem. A* **2003**, *107*, 107117.

(28) Becke, A. D. *Phys. Rev. Sect. A.* **1988**, *38*, 3098.

(29) Lee, C.; Yang, W.; Parr, R. G. *Phys. Rev. Sect. B.* **1988**, *37*, 785.

(30) Frisch, M. J.; Pople, J. A.; Binkley, J. S. *J. Chem. Phys.* **1984**, *80*, 3265.

(31) Woon, D. E.; Dunning, T. H., Jr. *J. Phys. Chem.* **1993**, *98*, 1358.

(32) Kendall, R. A.; Dunning, T. H., Jr.; Harrison, R. J. *J. Phys. Chem.* **1992**, *96*, 6796.

(33) Foresman, J. B.; Head-Gordon, M.; Pople, J. A.; Frisch, M. J. *J. Phys. Chem.* **1992**, *96*, 135.

(34) Mohamadi, F.; Richard, N. G. J.; Guida, W. C.; Liskamp, R.; Lipton, M.; Caufield, C.; Chang, G.; Hendrickson, T.; Still, W. C. *J. Comput. Chem.* **1990**, *11*, 440.

(35) Frisch, M. J. T.; G. W.; Schlegel, H. B.; Scuseria, G. E.; Robb, M. A.; Cheeseman, J. R.; Zakrzewski, V. G.; J. A. Montgomery, J.; Stratmann, R. E.; Burant, J. C.; Dapprich, S.; Millam, J. M.; Daniels, A. D.; Kudin, K. N.; Strain, M. C.; Farkas, O.; Tomasi, J.; Barone, V.; Cossi, M.; Cammi, R.; Mennucci, B.; Pomelli, C.; Adamo, C.; Clifford, S.; Ochterski, J.; Petersson, G. A.; Ayala, P. Y.; Cui, Q.; Morokuma, K.; Malick, D. K.; Rabuck, A. D.; Raghavachari, K.; Foresman, J. B.; Cioslowski, J.; Ortiz, J. V.; Baboul, A. G.; Stefanov, B. B.; G. Liu, A. L.; Piskorz, P.; Komaromi, I.; Gomperts, R.; Martin, R. L.; Fox, D. J.; Keith, T.; Al-Laham, M. A.; Peng, C. Y.; Nanayakkara, A.; Gonzalez, C.; Challacombe, M.; Gill, P. M. W.; Johnson, B.; Chen, W.; Wong, M. W.; Andres, J. L.; Gonzalez, C.; Head-Gordon, M.; Replogle, E. S.; Pople, J. A. Gaussian 98, Revision A.7. Gaussian, Inc.: Pittsburgh, PA, 1998.

(36) Plusquellic, D. F.; R.; Suenram, R. D.; Mate, B.; Jensen, J. O.; Samuels, A. C. *J. Chem. Phys.* **2001**, *115*, 3057.

(37) Hopkins, J. B.; Powers, D. E.; Smalley, R. E. *J. Chem. Phys.* **1980**, *73*, 683.

(38) Ribblett, J. W.; Borst, D. R.; Pratt, D. W. *J. Chem. Phys.* **1999**, *111*, 8454.